

CHARACTERIZATION STUDY OF DOUBLE FILTERED SENSOR LENGTH EFFECT ON STRAIN SENSITIVITY[†]

Wasmaa A. Jabbar^{a*}, Ayser Hemed^{a†}, Mayyadah Fadhala^{b‡}, Ismaeel Al-Baidhany^{a§}

^aDepartment of Physics, College of Education, Mustansiriyah University, Baghdad, Iraq

^bAlsalam Distinguished Students Secondary School, 2nd Karkh directorate of education, Baghdad, Iraq

[†]Corresponding author e-mail: ayser.hemed@uomustansiriya.edu.iq,

*E-mail: wasmaajabbar@uomustansiriya.edu.iq, ‡E-mail: mayads539@gmail.com; §E-mail: ismaeel_2000@uomustansiriya.edu.iq

Received April 15, 2023; revised June 7, 2023; accepted June 8, 2023

In this simulation study, Optisystem 18 software is used to monitor and study the effectiveness of side strain on selected lengths of two virtual uniform fiber Bragg grating (FBG) sensors. The operational FBG sensor Bragg wavelength was 1550 nm, which is used to find the measured shift in deflected light source optical spectrum. This value is also supplied by the light source to offer the minimum absorption and attenuation during transmission inside the optical fiber. Reliability of the sensor and technique of transferring the signal under such effect are screened. The investigation is also used to observe the shift in wavelength with altered applied side strain. The influence of sensor active length on side strain sensitivity is studied where according to theory, the length of the FBG influences the sensitivity via reflectivity R . The constructed sensor sensitivity is observed against length before and during the experiment. The sensing principle, in essence, depends on tracking the wavelength shift due to the variation of such strain. Results achieved in this study show an inverse relationship between sensor effective length and shift in the observed wavelength. The measured strain sensitivity is carried out for the active sensor length, which ranges from 0.05 to 15 cm, with corresponding sensitivity values of 1.19 pm/°C to 0.9 pm/°C, respectively, under the same strain conditions. The empirical results also show the success of the suggested sensing system in measuring strain. The strain measurement, ϵ , is linearly increasing, identical to the increasing values of the wavelength shift of Bragg. It's also been observed that the wavelength of Bragg is shifting during small ratios in the length protraction of the FBGs.

Keywords: Bragg-Grating; Elasto-Optic Effect; Optisystem; Strain-Sensor; Strain-Optic Tensor

PACS: 42.81.-i; 42.81. Pa

INTRODUCTION

Due to its properties such as; high sensitivity, small size, light weight, low price, material qualities, and sensing capabilities, optical fiber has emerged as a possible candidate for sensing applications. Other primary advantages of fiber optic sensors are chemical passivity, high temperature tolerance, immunity to electromagnetic interference, and long life with the possibility of usage in a hazardous environment [1]. Optical fiber sensors based on FBG technology, from the other hand, included additional advantages such as sensitivity, reliability, low intrusiveness, galvanic insulation, and the possibility to provide quasi-distributed remote measurements. FBGs are extensively utilized in optical sensing and can compete with traditional electrical strain gauges. To determine many parameters such as temperature, strain, refractive index, pressure, etc. FBGs also have many applications in civil engineering and aeronautics [2]. Furthermore, FBG sensors have received widespread recognition for features such as erosion resistance, immunity to electromagnetic and radio frequency interference, and the ability to operate in harsh environments where traditional sensors cannot [3]. For the time being, many interferometry techniques, including Mach-Zehnder and Fabry-Perot, have been suggested for heat sensing implementation [4]. From the other hand, applications with FBGs includes in additional to sensing, laser experiments for chaotic generation in parallel to sensing such as studies listed in Refs. [5] [6] [7].

THEORETICAL APPROACH

Despite the rotating cross-section of an optical fiber, examine only an average stack, in that the doubled layers are distinct with indices of interleaved of refraction n_1 and n_2 , for core and cladding, respectively, where n_1 differs from n_2 in magnitude to ensure the light guiding [8]. A light beam possessing monochromatic wavelength perpendicularly launches into the stack. Suppose the thickness of all medium layer is controllable, one may discover once the thickness of each layer reaches $\lambda_B/4$, in where λ_B is the relative wavelength in the medium, or $\lambda_B = \lambda_o/n_{avr}$. where n_{avr} . is the average index of refractive of the intermediate stack, such that all the reflected waves of light from the stack interfere constructively at the interface where light is injected and give rise to a substantial reflection at wavelength λ_B . If the number of layers is sufficient, and/or the medium stacks refractive index modulation becomes deeper, eventual reflection will approach unity at λ_B . Subsequently, if the above depicted refractive index grating is constructed in the center of the optical fiber, a fiber Bragg grating is produced.

For a single mode fiber, the only mode propagating is LP₀₁, if the fiber grating pitch is known as the thickness of double layers of neighboring, the FBG condition (first order condition [1]) can then be expressed as [9]:

$$\lambda_B = 2n_{eff}\Lambda \quad (1)$$

where n_{eff} is the effective core index of refraction for fundamental mode.

[†] Cite as: W.A. Jabbar, A. Hemed, M. Fadhala, I. Al-Baidhany, East Eur. J. Phys. 3, 509 (2023), <https://doi.org/10.26565/2312-4334-2023-3-58>

© W.A. Jabbar, A. Hemed, M. Fadhala, I. Al-Baidhany, 2023

A portion of the propagating light scatters at each grating plane, which causes the scattered light to either transmit or reflect at the grating planes. Destructive interference causes the reflected beams to cancel each other out if they are out of phase. The reflected wave constructively interferes and back-reflects, satisfying the Bragg condition, when the light rays reflected from each grating plane are in phase [1].

The influences of strain on a fiber grating have two-fold; firstly, the alteration in physical spacing between sequential index amendments (fiber grating pitch) will cause a shift of λ_B and, secondly, the strain-optic influence will induce an alteration in the index of the refraction causing additional shift of λ_B . Because of this, a technique to gauge temperature and strain fluctuations has been made possible by changes in these two physical characteristics [1]. Periodic difference in Λ inside the FBG, and the index of refractive affected the deflected wavelength [11]. Altering in last grating parameter due to strain is calculated by the following Equation [10]:

$$\Delta\lambda_B = 2 \left[\Lambda \frac{\partial n_{eff}}{\partial l} + n_{eff} \frac{\partial \Lambda}{\partial l} \right] \Delta l \quad (2)$$

where $\Delta\lambda_B$ is the change in Bragg's wavelength and l is the effective length.

Last equation measures the strain influence on the FBG. This matches the influence of the grating spacing and the strain-optic induced influence in index of refraction [8]. Under the case of a uniform strain along the axis of the optical fiber and no temperature alteration, the shift of wavelength is linked to the strain (ε_z) by the coefficient of elastic-optical (ρ_e) [8] [10]:

$$\Delta\lambda_B = \lambda_B(1 - \rho_e)\varepsilon_z \quad (3)$$

Equation (3) indicates that in the Bragg peak shift of wavelength is proportional to applied strain. In the sensing theory of FBG, the strain value ε_z should be expressed as

$$\varepsilon_z = \frac{\Delta\lambda_B}{\Delta\lambda_B(1-\rho_e)} \quad (4)$$

where ε is the strain direction along the lengthwise of the fiber, ρ_e is calculated as the following [11]:

$$\rho_e = \frac{n_{eff}^2}{2[\rho_{12}-v(\rho_{11}+\rho_{12})]} \quad (5)$$

here ρ_{11} and ρ_{12} are components of the strain-optic tensor, and v is the ratio of Poisson. For a model Germanium-Silicate optical fiber, parameters for last equation are reported in Ref. [11] as the following: $\rho_{11} = 0.113$, $\rho_{12} = 0.252$, $v = 0.16$ and $n_{eff} = 1.482$.

A Bragg grating region is a result of a permanent periodic refraction index modulation in the core area of an optical fiber when exposure to UV. The phenomenon of a permanent refractive index change is called photosensitivity, to enhance this effect Germanium is doped into fiber core [1]. The magnitude of the change is also affected by the intensity and duration of the exposure. The operations principle of an FBG sensor are observed by observing the shift in wavelength of the output signal with the variations in the measurement as strain or the light reflected heat using an FBG [12].

There are various kinds of sensors obtainable using optical fiber. It is classified into three kinds: extrinsic, intrinsic, and hybrid [13]. The optical characteristics of intrinsic type are sensitive to strain and temperature [14]. For the information transition to a long-range site, extrinsic is the better option [15] [1]. Here, the length of the FBG influences the sensitivity via reflectivity R , which is itself function to length of FBG and light wavelength according to the following Equation [1]:

$$R(l, \lambda) = \frac{\Omega^2 \sinh^2(sl)}{\Delta k^2 \sinh^2(sl) + s^2 \cosh^2(sl)} \quad (6)$$

where Δk is detuning of wave vector and Ω is a coupling coefficient.

Thus, length term (l) in last equation indicate an important factor of the grating when determining its sensitivity. Different groups studied the relationship between the grating length and the sensitivity. When the direction of the highest strain is parallel to the fiber axis, the sensitivity of FBGs to strain in the static is greatest, and it is least sensitive when it is orthogonal to the axis [16]. According to Liang Ren et al., the lateral strain can be neglected in comparison with the longitudinal strain of the fiber [17]. Frieden *et al.* reported that the longitudinal strain predominates on the optical fiber, and the transverse strain sensed by the optical fiber is six times smaller than the surrounding transverse strain, also known as a transverse or traction transverse bending [16].

Ref. [1] has developed FBG sensors which may be applied to scale the kinematics of body, by using optisystem program software. This mode, huge long sensors, is wearable system that may watch most knee flexibility, motion, and all the alterations during the full period of human motion [18].

Based on that, it is very desirable to discuss the variation of the strain sensitivity of FBG sensor systems with a selected sensor length. This work represents an attempt to fulfill such a demand and also to develop a systematic approach for deciding the sensor length corresponding to an application. The focus of this study is to analyze the execution of the sensor while it is being used with a certain strain. Hence, the values of strain that can be applied to analyze the most useful values of strain that can be used on the FBG. The paper calculations were all completed by applying simulation with the software "Optisystem version 18" with the consideration for specific light source wavelength.

SIMULATION SET-UP

As shown in Fig. (1), the set-up includes one source of white light, its light is launched into a single mode fiber with 60 Km length. Two uniform FBG sensors, with $\lambda_B = 1550 \text{ nm}$ receives the light. These two sensors subject to selected values of longitudinal strain, named "zz". Two optical nulls are used to close the effect of back-reflected portion or transmitted light. Observations were recorded by using two optical spectrum analyses and three FBG sensors investigator. FBG 1 can respond to both heat and strain whilst FBG 2 sensors is for only for scaling temperature. The FBG investigator is for display the shift of wavelength from the reflecting spectra of both two FBG sensors, separately. Strain is selected to vary from the value 0.005 to 0.01. All remaining parameters in the Optisystem software follow their default setting.

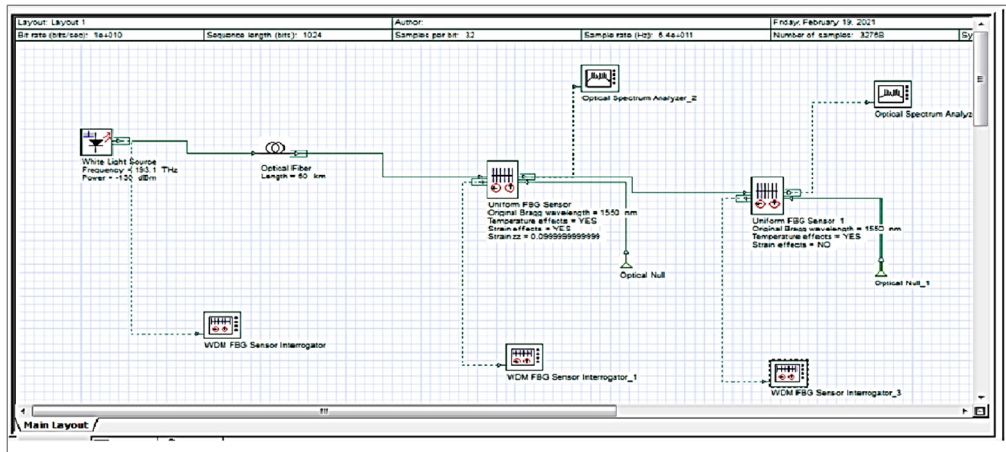


Figure 1. Simulation set-up for double-filtered FBG sensor design

RESULTS AND DISCUSSIONS

The results are obtained by applying six various values of strain to analyze the effectiveness of axial strain on FBG. The resulted shift in peak wavelength decreased with an increase in axial strain value. For comparisons, the theoretical computation of sensitivity was first performed by applying Equation (3) for the value of temperature (3°C) and strain. Results for the theoretical computation of peak shift by wavelength are shown in Tables (1, 2, and 3) for wavelengths of 1550, 1310, and 980 nm, respectively.

From Figure (2), we found that the sensitivity for each wavelength was different from the other, but the largest sensitivity was found with $\lambda=1550 \text{ nm}$ which equals 53 pm/pe, so the sensor of wavelength, 1550 nm, was chosen to make a simulation in this work.

Table 1. Computation for peak wavelength shift with 1.550 um.

Initial wavelength λ_B (um)	Temperature (°C)	Strain experienced by FBG	Peak wavelength shift (nm)
1550	3	0.0051	6.63820
		0.0061	7.96584
		0.0071	9.29348
		0.0081	10.6211
		0.0091	11.9487
		0.01	13.2764

Table 2. Calculation of peak wavelength shift with 1310 nm.

Initial wavelength λ_B (nm)	Temperature (°C)	Strain experienced by FBG	Peak wavelength shift (nm)
1310	3	0.005	5.61035
		0.006	6.73242
		0.007	7.85449
		0.008	8.97656
		0.009	10.0986
		0.01	11.2207

Table 3. Calculation of peak wavelength shift with 980 nm.

Initial wavelength λ_B (nm)	Temperature (°C)	Strain Experienced by FBG	Peak wavelength shifted (nm)
980	3	0.005	4.1970
		0.006	5.036
		0.007	5.875
		0.008	6.715
		0.009	7.554
		0.01	8.394

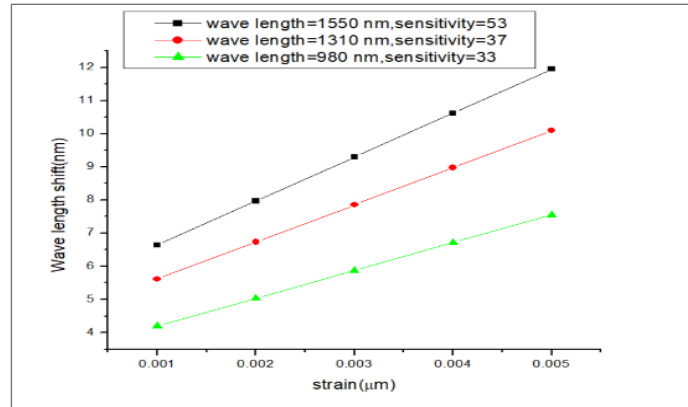


Figure 2. Results for peak wavelength shift experienced by FBG versus strain.

Measured results for wavelength peak shifting according to simulations are given in Table 4. Fig. 3 displays shifting of wavelength against strain experienced by FBG, theoretically. Sensor sensitivity shows directly proportional with increasing of FBG active length within the range (0.05-15 cm). Also increasing the FBG active length shows linear relation between wavelength shift as with applied strain variation showed in the same figure. Fig. 4 displays wavelength peak shift against strain experienced by FBG via simulation. Figure 5 displays comparison between the theoretical calculations and simulation results of the peck shifted of wavelength. The FBG sensor in Optisystem also has strain value limitation that cause the wavelength were shifting when the value of strain changed.

Table 4. Results for peak wavelength shift calculations by simulation

Initial wavelength λ_B (nm)	Temperature change ($^{\circ}\text{C}$)	Strain experienced by FBG	Peak wavelength shifted (nm)
1550	3	0.0051	3.370
		0.0061	4.054
		0.0071	4.718
		0.0081	5.392
		0.0091	6.000
		0.01	6.740

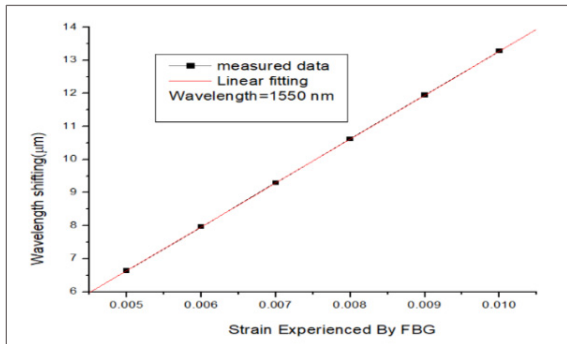


Figure 3. Results for theoretical calculations of shifted-wavelength against strain experienced by FBG

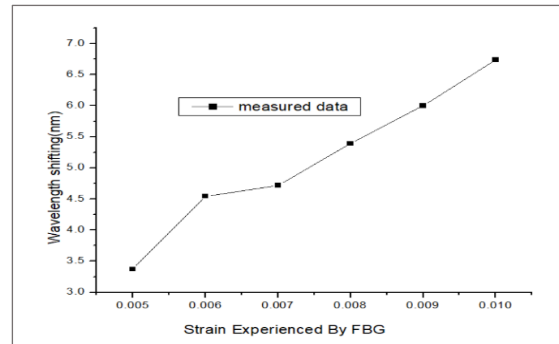


Figure 4. Wavelength peak-shift against the strain experienced by FBG (simulations)

From the Figure (5), the values of simulation and theory weren't the same due to the design of the parameter groups in the simulation software. In addition, there was a special optical fiber composition used in the simulation that could influence the wavelength values via dispersion, as mentioned in theory as material dispersion relations, such as Ref. [19]. Furthermore, the effects of the shift in wavelength in a Bragg grating engraved in fiber with a diameter of 125 μm and the index of effective index $n_{eff} = 1.4473$. This result agrees will with experimental work reported by Ref. [20], while simulation results present better behaviors than theoretical calculations in comparison with Ref. [21].

Figure 5 shows the relationship between wavelength shift of three different values of wave lengths and strain of six different values. This work searches for the influence of the length of the sensor on the strain sensitivity of the FBG. Sensitivity for grating region protection, pre-tensioning, the adhesive of the sensor, and the choice of length of the sensor are based on experimental work presented by Ref. [22]. Concerns examined before and during the experimentation structure of an FBG sensor.

In general, an FBG sensor can be made in any length, where for every measurement, the system resolution defines the potential accuracy and precision of its performance. For an FBG sensor system, the strain-to-length relationship is shown in Figure 6. This is an inverse relationship between sensor length and strain. It is concluded that an integer multiplied by the FBG effective length of a longer sensor has a better strain resolution. If the monitoring requirements have a resolution of 1 $\mu\text{m}/\mu\text{e}$ suggested sensor active length will

be (0.05 to 0.15) cm. If the size of the structure is relatively small, then a compromise has to be made between the sensor resolution and gauge length.

According to the operating principle, the grating reflects the various wavelength components of the signal at various points along the grating. Also, it's clear from the transportation that the Bragg wavelength results and the shift of Bragg wavelengths are progressively increased with increased loading. If the used loading is uniform, then the shifting of wavelengths by Bragg happens without amendment to the initial form of the spectrum. The strain of the 0.05 cm sensor was studied versus all results of shifted Bragg wavelengths applied in simulation, as shown in Figure 7. When it is regular, shifts take place without adjustment of the initial spectrum form. The strain is determined from the shift in wavelengths acquired under the used loading. The strain measurement ϵ , obtained after computation, is linearly increasing, identical to the increasing shifted Bragg wavelength value. So, a plot between the Bragg wavelength shift and the strain for a 0.05 cm sensor is drawn as a straight line.

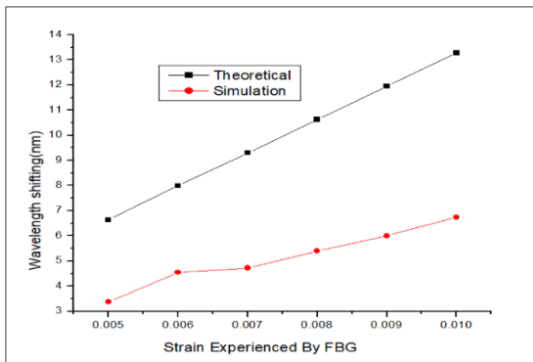


Figure 5. Comparisons between and the simulation and theoretical shifted of wavelength

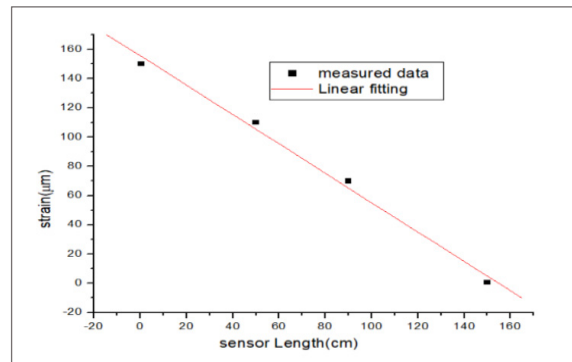


Figure 6. Strain resolution of the FBG sensor (sensor accuracy)

After application of longitudinal tense to FBG, during the test, the first and last identical transmission spectra observed by the optical spectrum analyzer are displayed to proceed the shift of the Bragg wavelength. An alteration in load with sensor length equal to 15 cm is observed in this experiment, as displayed in Fig. 8.

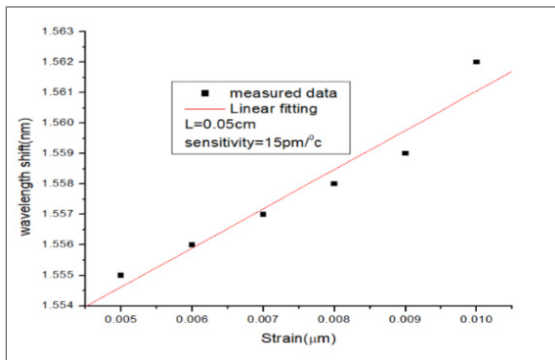


Figure 7. Shift of Wavelength against used strain for the 0.05 cm sensor (simulation)

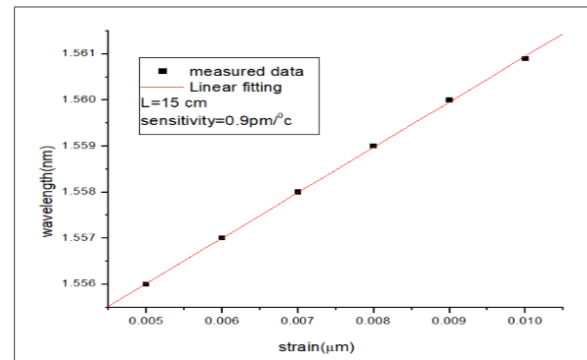


Figure 8. Shift of wavelength against applied strain for the 15 cm sensors length

During the simulation run, the strain measurement for the 15 cm long sensor was studied versus each value of wavelength shift. The strain measurement, ϵ , is linearly increasing, identical to the increasing values of the wavelength shift of Bragg. It's also been observed that the wavelength of Bragg is shifting during small ratios in the length protraction of the fiber gratings.

This test is carried out for two different lengths of grating, which are 0.05 and 15 cm. Analysis of the optical spectra was done for the detected signal of Bragg wavelength. Figure 9 shows the relation between wavelength shift and intensity for the wavelengths of 1550 nm, 1310 nm, and 980 nm on strain sensitivity.

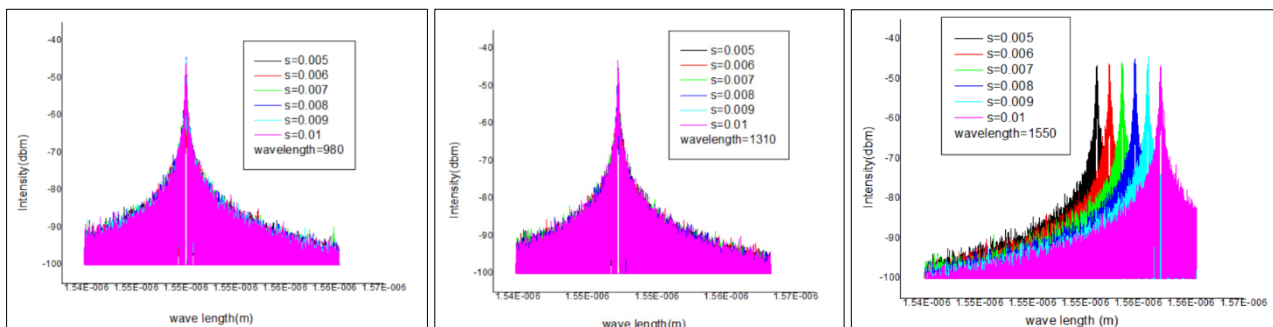


Figure 9. Relation between intensity and wavelength shift for; 1550, 1310 and 980 nm for mentioned strains

CONCLUSIONS

According to the consequence of simulations, shifted wavelengths have been observed with several active lengths for virtual FBGs. Comparisons for observations based on theoretical calculations are carried out indicates that there is only a little variation between simulation and theoretical results. Based on the FBG sensors suggested in the experiment, the consequences show that efficient length is inversely related with shift in Bragg wavelength when axial strain increased. This means FBG sensor is most sensitive to the shortest FBG sensor length and less sensitive to the largest length of sensor due to the complicated math effect of reflectivity R parameter. It's also concluded from the relationship of the theoretical computation against empirical values and then the linearity of the strain against the shifted wavelength of Bragg that it may be applied in implementations in optical sensing as a sensor of high heat, a sensor of fire alarm, a sensor of vibration, or a sensor of pressure.

Acknowledgments

The authors would like to thank Mustansiriyah University (www.uomustansiriyah.edu.iq) and Ministry of Science and Technology, Baghdad, Iraq for their support in the present work.

ORCID

© Wasmaa A. Jabbar, <https://orcid.org/0000-0003-3966-9468>; © Ayser Hemed, <https://orcid.org/0000-0003-0319-1650>
© Ismaeel Al-Baidhany, <https://orcid.org/0000-0001-5273-9921>

REFERENCES

- [1] N. Dedyagala, PhD. Dissertation, Optical Fiber Bragg Grating Analysis Through FEA and its Application to Pressure Sensing, College of Engineering and Science, Victoria University, 2019.
- [2] B.A. Tahir, M.A. Saeed, A. Ahmed, S.M.Z. Iqbal, R. Ahmed, M.G.B. Ashiq, H.Y. Abdullah, and R.A. Rahman, *Chinese Journal of Physics*, **49**(5), 1035-1045 (2011).
- [3] G. Zhou, L.M. Sim, and J. Loughlan, *Smart Materials and Structures IOP Publishing Ltd*, vol. 13, no. 6, p. 1291, (2004), <https://doi.org/10.1088/0964-1726/13/6/003>
- [4] N. S. Sahidan, M. A. M. Salim, S. S. Osman, H. Bakhtiar, N. Bidin, G. Krishnan, M. H. D. Othman, M. A. Rahman, A. F. Ismail and N. Yahya, in *International Laser Technology and Optics Symposium 2019 (iLATOS2019)*, (2019, Senai, Malaysia), <https://doi.org/10.1088/1742-6596/1484/1/012015>
- [5] Z.R. Ghayib, and A.A. Hemed, Springer Link, *Pramana - J Phys*, **96**(86), (2022), <https://doi.org/10.1007/s12043-022-02305-2>
- [6] Z.R. Ghayib, PhD. Dissertation, Controlling a chaotic synchronization by modified FBG sensor, College of Education, Mustansiriyah University, 2022.
- [7] Z.R. Ghayib, and A.A. Hemed, "Smart Control For The Chaotic Dynamics Using Two Regions Uniform Fiber Bragg Grating," *Optoelectronics and Advanced Materials-Rapid Communications*, **16**, 307-318, (2022), <https://oam-rc.inoe.ro/articles/smart-control-for-the-chaotic-dynamics-using-two-regions-uniform-fiber-bragg-grating>
- [8] S. Cheng, W. Hu, H. Ye, L. Wu, Q. Li, A. Zhou, M. Yang, Q. Zhao, and D. Guo, *Optics Express*, **29**(22), 35765-35775 (2021). <https://doi.org/10.1364/OE.441896>
- [9] M.I.M. Razi, M.R.C. Beson, S.N. Azem, and S.A. Aljuni, *Indonesian Journal of Electrical Engineering and Computer Science*, **14**(2), 564-572 (2019). doi: <http://doi.org/10.11591/ijeecs.v14.i2.pp564-572>
- [10] M.M. Werneck, R.C.S.B. Allil, B.A. Ribeiro, and F.V.B.D. Nazaré, "A Guide to Fiber Bragg Grating Sensors," in *Current Trends in Short- and Long-period Fiber Gratings*, London, UK, Edited by Christian Cuadrado-Laborde (IntechOpen 2013), pp. 7-8.
- [11] Othonos, and K. Kalli, *Fiber Bragg Gratings: Fundamentals and Applications in Telecommunications and Sensing* (Artech House Optoelectronics Library) Illustrated Edition, vol. 53, (Artech House Print on Demand, 1999).
- [12] E. Al-Fakih, N.A.A. Osman, and F.R.M. Adikan, *Sensors (Basel)*, **12**(10), 12890-12926 (2012), <https://doi.org/10.3390/s121012890>
- [13] Razzaq, H. Zainuddin, F. Hanaffi, and R.M. Chyad, *IET Science, Measurement & Technology*, **13**(5), 615-621 (2019). <https://doi.org/10.1049/iet-smt.2018.5076>
- [14] M. Boerkamp, D.W. Lamb, and P.G. Lye, in *Journal of Physics: Conference Series, Volume 76, Sensors and their applications XIV 11–13 September 2007, Liverpool John Moores University*, Liverpool, UK, 2007.
- [15] P.C. Beard, and T.N. Mills, *Applied Optics*, **35**(4), 663-675 (1996). <https://doi.org/10.1364/AO.35.000663>
- [16] Z. Fang, K. Chin, R. Qu, H. Cai, and K. Chang, *Fundamentals of Optical Fiber Sensors*, (Wiley Series in Microwave and Optical Engineering 2012).
- [17] L. Huo, H. Cheng, Q. Kong, and X. Chen, *Sensors*, **19**, 1231 (2019), <https://doi.org/10.3390/s19051231>
- [18] R.P. Rocha, A.F. Silva, J.P. Carmo, and J.H. Correia, "FBG in PVC foils for monitoring the knee joint movement during the rehabilitation process," in *33rd Annual International Conference of the IEEE EMBS*, <https://doi.org/10.1109/IEMBS.2011.6090064> (Boston, Massachusetts USA, 2011) pp. 458-461
- [19] Hemed, MSc. Thesis, Studying the Effective Factors on Producing Modal Birefringence (High and Low) in the Single Mode Optical Fiber, College of Education, Mustansiriyah University, 2005.
- [20] S.M. Khorsheed, A.A. Hemed, and M.M. Fdhala, *World Scientific News*, **137**, 42-57 (2019), <http://www.worldscientificnews.com/wp-content/uploads/2019/09/WSN-137-2019-42-57.pdf>
- [21] M.M. Fdhala, and S.M. Khorsheed, *European Journal of Advances in Engineering and Technology*, **7**(2), 1-6 (2020). <https://ejaet.com/archive/volume-7-issue-2-2020>
- [22] A.A. Hemed, M.M. Fdhala, and S.M. Khorsheed, *Kuwait J. Sci.* **49**(1), 1-18 (2022). <https://doi.org/10.48129/kjs.v49i1.12487>

**ХАРАКТЕРИСТИЧНЕ ДОСЛІДЖЕННЯ ВПЛИВУ ДОВЖИНИ ДАТЧИКА З ПОДВІЙНИМ ФІЛЬТРОМ
НА ЧУТЛИВІСТЬ ДО ДЕФОРМАЦІЙ****Васма А. Джаббар^а, Айсер Хемед^а, Майяда Фадхала^б, Ісмаїл Аль-Байдхані^а**^а*Департамент фізики, педагогічний коледж, університет Мустансірія, Багдад, Ірак*^б*Середня школа Алсаламу, управління освіти Карха, Багдад, Ірак*

У цьому моделювальному дослідженні програмне забезпечення Optisystem 18 використовується для моніторингу та вивчення ефективності бокової деформації на вибраних відрізках двох віртуальних однорідних волоконних датчиків Брегга (FBG). Довжина хвилі робочого датчика FBG Брегга становила 1550 нм, що використовується для визначення виміряного зсуву в оптичному спектрі відхиленого джерела світла. Це значення також забезпечується джерелом світла, щоб забезпечити мінімальне поглинання та ослаблення під час передачі всередині оптичного волокна. Перевірено надійність датчика та техніку передачі сигналу при такому впливі. Досліджування також використовується для спостереження за зсувом довжини хвилі зі змінним прикладеним боковим натягом. Досліджується вплив активної довжини датчика на чутливість до бокової деформації, де, згідно з теорією, довжина FBG впливає на чутливість через відбивну здатність R. Побудовану чутливість датчика спостерігалась відносно довжини до та під час експерименту. Принцип чутливості, по суті, залежить від відстеження зсуву довжини хвилі через зміну такої деформації. Результати, отримані в цьому дослідженні, демонструють обернену залежність між ефективною довжиною датчика та зміщенням спостережуваної довжини хвилі. Виміряна чутливість до деформації проводиться для довжини активного датчика, яка коливається від 0,05 до 15 см, з відповідними значеннями чутливості від 1,19 пм/°C до 0,9 пм/°C, відповідно, за однакових умов деформації. Емпіричні результати також показують успішність запропонованої системи вимірювання деформації. Вимірювана деформація, ϵ , лінійно зростає, ідентично зростаючим значенням зсуву довжини хвилі Брегга. Було також помічено, що довжина хвилі Брегга зміщується під час малих коефіцієнтів подовження довжини FBG.

Ключові слова: *решистка Брегга; еластооптичний ефект; Optisystem; сенсор напруги; деформаційно-оптичний тензор*